

## Phonon modes in Si [111] nanowires

T. Thonhauser<sup>1</sup> and G. D. Mahan<sup>1,2</sup>

<sup>1</sup>*Department of Physics, Pennsylvania State University, University Park, Pennsylvania 16802, USA*

<sup>2</sup>*Materials Research Institute, Pennsylvania State University, University Park, Pennsylvania 16802, USA*

(Received 18 November 2003; published 27 February 2004)

We solve a long standing question concerning the boundary conditions for optical phonons in nanowires. The controversy between the so-called *clamped* and *free* conditions is well documented in standard literature. We answer this question of the boundary conditions by presenting a spring-and-mass model of the Stillinger and Weber type to calculate optical and acoustic phonons in Si [111] nanowires. Our results show that this model, in parallel to the bulk case, is sufficient to describe important features of the phonon spectrum. Furthermore, our results predict that optical phonons in nanowires are subject to clamped boundary conditions.

DOI: 10.1103/PhysRevB.69.075213

PACS number(s): 63.22.+m, 43.20.+g, 62.30.+d, 63.20.Dj

### I. INTRODUCTION

Over the last decades nanostructures have become a field of intense study, not only experimentally but also from a theoretical point of view. One field of interest deals with phonon modes in nanotubes and nanowires.<sup>1-3</sup> Despite the fact that a lot of research has been done in this field, a controversy about the boundary conditions of optical phonon modes in nanowires has arisen. Two different possibilities, i.e., the so-called *clamped* and *free* boundary conditions, are discussed in the literature.<sup>4-10</sup> Motivated by this discrepancy, we performed numerical calculations on optical phonons in a Si [111] nanowire in order to solve this longstanding question.

### II. THEORY

Sound waves are acoustical phonons of long wavelength. They can be calculated using classical elasticity theory and the boundary conditions are well known.<sup>2,11</sup> The vibrational modes of an infinite cylinder are described in standard texts.<sup>11-13</sup> A similar classical analysis is possible for optical phonons of long wave length. In this case, the dynamical equation must have a term of the order  $\mathcal{O}(q^2)$ , where  $\mathbf{q}$  is the wave vector of the phonon. The frequency equation at long wavelength for an optical phonon of amplitude  $Q_\mu$  ( $\mu = x, y, z$ ) can be written as

$$\omega(q)^2 Q_\mu = \omega_0^2 Q_\mu + \omega_c^2 t_{\mu\nu}(\mathbf{q}) Q_\nu - F_{\mu\nu\alpha\beta} q_\alpha q_\beta Q_\nu. \quad (1)$$

The first term on the right-hand side of Eq. (1) is due to the short-range forces between the nearby neighbors. This is an isotropic interaction in cubic crystals. The second term is due to the long-range dipolar interaction. It provides the splitting between LO and TO phonons and in three-dimensional cubic crystals it has the form

$$t_{\mu\nu}(\mathbf{q}) = 3 \frac{q_\mu q_\nu}{q^2} - \delta_{\mu\nu}. \quad (2)$$

This functional form will change in a nanowire, since the sum over dipolar interactions is essentially one dimensional.<sup>14</sup> The last term in Eq. (1) is the quadratic term in the wave vector mentioned above. The fourth-rank tensor

$F_{\mu\nu\alpha\beta}$  is determined by group theory. In the case of cubic crystals  $F$  is found to have three independent constants, similar to elastic constants, which are called  $f_{11}$ ,  $f_{12}$ , and  $f_{44}$  in Voigt notation. For silicon we find that  $\omega_c^2 = 0$  and therefore we can write the actual equation as

$$\begin{aligned} \frac{\partial^2}{\partial t^2} Q_x = & -\omega_0^2 Q_x - f_{11} \frac{\partial^2 Q_x}{\partial x^2} - f_{44} \left( \frac{\partial^2}{\partial y^2} + \frac{\partial^2}{\partial z^2} \right) Q_x \\ & - (f_{12} + f_{44}) \frac{\partial}{\partial x} \left( \frac{\partial Q_y}{\partial y} + \frac{\partial Q_z}{\partial z} \right). \end{aligned} \quad (3)$$

Cyclic permutations give similar equations for  $Q_y$  and  $Q_z$ . The choice of sign in front of the constants  $f_{ij}$  is determined by the expectation that  $f_{ij} > 0$  for most solids. For isotropic systems the relation  $2f_{44} = f_{11} - f_{12}$  holds and Eq. (3) becomes

$$\frac{\partial^2}{\partial t^2} Q_\mu = -\omega_0^2 Q_\mu - f_{44} \nabla^2 Q_\mu - (f_{11} - f_{44}) \nabla_\mu (\nabla \cdot \mathbf{Q}). \quad (4)$$

This equation has an obvious similarity to the wave equation for sound waves. The vector amplitude  $Q_\mu$  in Eqs. (3) and (4) requires three boundary conditions on each surface. Here the question arises as to what are the boundary conditions for optical phonons in a nanowire? The “free” conditions ensure that the surface of the nanowire is stress free, whereas the “clamped” conditions mean  $\mathbf{Q} = 0$  all around the surface. In general, these possibilities contradict.

In order to answer this question, we used a spring-and-mass model to calculate phonon modes in a Si [111] nanowire. All previous calculations of phonons in wires have used the isotropic model mentioned above. In contrast to this we used a crystalline model. We utilized a parametrization by Keating,<sup>15</sup> which is a special case of the well-known Stillinger and Weber model.<sup>16</sup> This model has been proved to be accurate and sufficient to describe phonon spectra and related quantities of materials that crystallize in the diamond structure. Within this model, the dynamical equation for particle  $i$  with amplitude  $\mathbf{Q}^i$  can be written as

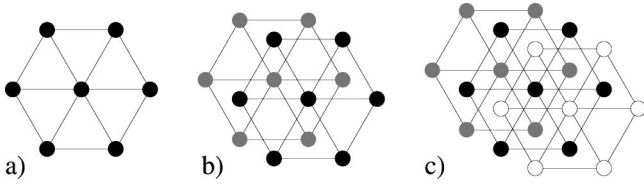


FIG. 1. Approximation for a Si [111] nanowire by a hexagon shaped cross section. Depicted are the placings of the first two layers as black spheres (a), the two middle layers in gray color (b), and the last two layers as white spheres (c). The line of sight parallels the  $z$  direction, which also forms the axis of the nanowire.

$$M \frac{\partial^2}{\partial t^2} Q_\mu^i = - \frac{\partial U}{\partial Q_\mu^i}, \quad (5)$$

where  $M$  is the same mass for all particles. The potential  $U$  consists of two parts. The first part describes the interaction of particle  $i$  with its four nearest neighbors. The second term deals with the bond bending of the bonds between particle  $i$ ,  $j$  and  $i$ ,  $k$ . Thereby,  $j$  and  $k$  are confined to the tetrahedron in the center of which particle  $i$  is placed. Note that this interaction constitutes a three-body force. The interactions can be written as

$$U_{\text{n.n.}} = \alpha \sum_i^N \sum_{j=1}^4 [\mathbf{R}^{ij} \cdot (\mathbf{Q}^i - \mathbf{Q}^j)]^2, \quad (6)$$

$$U_{\text{b.b.}} = \beta \sum_i^N \sum_{j,k>j}^4 \left[ \cos \theta_{jik} + \frac{1}{3} \right]^2, \quad (7)$$

where  $N$  is the number of particles,  $\mathbf{R}^{ij}$  is a unit vector connecting the equilibrium positions of particles  $i$  and  $j$ , and  $\theta_{jik}$  is the angle between the two bonds  $i$ ,  $j$  and  $i$ ,  $k$ . The model includes two parameters  $\alpha$  and  $\beta$ , which determine the “strength” of  $U_{\text{n.n.}}$  and  $U_{\text{b.b.}}$ . We solved the model for the Si bulk material and fitted the bulk spectrum<sup>17</sup> with the two model parameters. Next, we applied the model to a Si nanowire, using the same ratio for  $\alpha/\beta$ . Note that in case of a wire, atoms on and near the surface might not necessarily have four nearest neighbors.

### III. COMPUTATIONAL DETAILS

Silicon nanowires grow naturally along the [111] direction, which we also chose to be the  $z$  axis of our coordinate system. In this configuration the Si atoms form hexagonal layers perpendicular to the  $z$  direction, similar to the case of close-packed spheres.<sup>18</sup> For our calculations we approximated the cross section of the nanowire by a hexagon. The six layers of Si atoms in the unit cell are now constructed as depicted in Fig. 1. Two layers of hexagons are stacked directly atop of each other (a). The next two layers are shifted, so that the atoms appear in the spaces between the atoms of the first layer (b). The last two layers are shifted again, so that the atoms cover the remaining empty sites (c). There are several choices for the placing of the last two layers with respect to the first four. For our calculations we chose an arrangement in which the center of mass is located in the

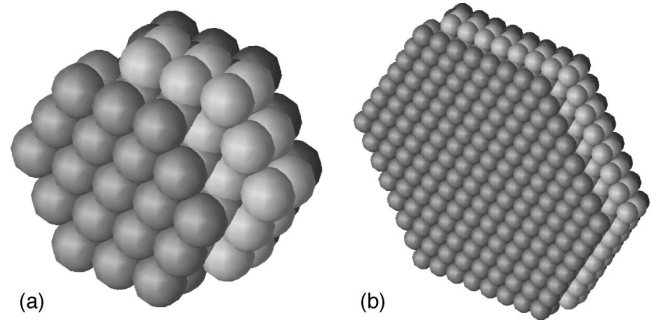


FIG. 2. Unit cell of a Si nanowire along the [111] direction. Each unit cell consists of 6 layers in the hexagonal structure. Depicted are a unit cell with two rings of atoms (a) and with seven rings of atoms (b). For better visualization, the groups of different layers are colored in different gray scales.

middle of the first layer, which then also defines the axis of the nanowire. The nanowire shown in Fig. 1 is rather small, since it has only three atoms across its diameter. We will refer to this system as a unit cell with *one ring* of atoms, since the hexagon in Fig. 1(a) has one atom in the center and one ring of atoms around the center one. This nomenclature provides an easy mechanism for creating bigger nanowires. In order to “grow” larger diameters, we simply add more rings of atoms. Figure 2 depicts different unit cells with two (a) and seven (b) rings. The distance between two Si atoms is approximately 0.384 nm. A wire with ten rings would therefore have 21 atoms across its cross section, i.e., 8 nm. In order to grow a 50 nm wire, 131 atoms have to be arranged along the diameter, i.e., 65 rings. For our calculations we considered wires with a number of rings from one to seven. Bigger values are impracticable due to the huge resulting matrix size. A unit cell with seven rings already consists of 1014 atoms, which results in a dynamical matrix the size of  $3042 \times 3042$ .

### IV. RESULTS

As mentioned above, the model used contains two parameters  $\alpha$  and  $\beta$ . For our calculations of the Si [111] nanowire phonon spectrum, the same ratio  $\alpha/\beta$  was utilized as found for the Si bulk material. The remaining degree of freedom was fitted so that the highest optical phonon with  $\mathbf{q}=0$  lies at 15.3 THz, i.e., the value for the bulk material.<sup>17</sup> For nanowires, only the wave vector along the axis of the wire is of interest. Henceforth, we abbreviate  $\mathbf{q}=(0,0,q_z)$  with  $q$ . Part of the phonon spectrum for a Si [111] nanowire with seven rings of atoms is depicted in Fig. 3. The entire spectrum consists of 3042 branches according to the 1014 atoms in the unit cell. The spectrum shows four acoustic branches characterized by  $\lim_{q \rightarrow 0} v_i(q) = 0$ , where  $v_i(q)$  is the frequency of mode  $i$  for the wave vector  $q$ . Two of these branches are linear in  $q$  and can therefore be identified as the longitudinal and transverse acoustical phonons. The transverse phonon is a torsional mode in the wire. Furthermore, two branches proportional to  $q^2$  can be observed, which are characteristic for wires. From the linear modes we calculated longitudinal and transversal sound velocities and the results are depicted in

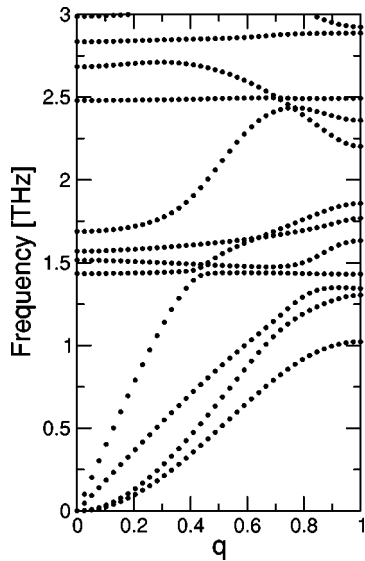


FIG. 3. Some low frequencies of the phonon spectrum for a Si [111] nanowire.  $q$  thereby refers to the reduced wave vector. Four acoustic branches are clearly visible. Two acoustic modes linear in  $q$  (longitudinal and transversal), but also two modes proportional to  $q^2$ , which are characteristic for wires.

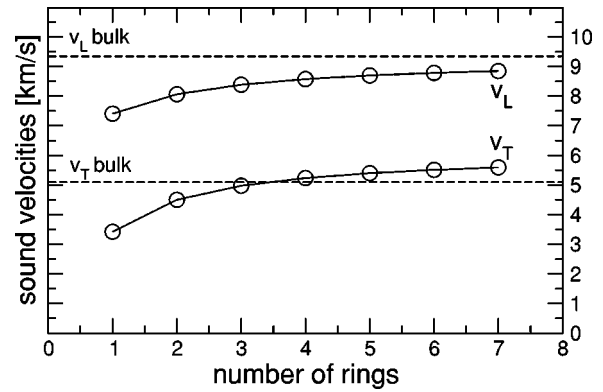


FIG. 4. Sound velocities  $v_L$  and  $v_T$  of the longitudinal and transversal acoustic modes in a Si nanowire along its axis. The velocities increase with the diameter of the wire, i.e., the number of rings used in the cross section. The corresponding bulk values for Si along the [111] direction are 9.35 and 5.09 km/s, which are marked by the broken lines.

Fig. 4. The sound velocities can be fitted to a  $1/r$  behavior. Using this parameterization, the limits for a large number of rings can be calculated and we find:  $v_L \rightarrow 9.3$  and  $v_T \rightarrow 6.1$  km/s. Concerning longitudinal sound waves, a wire with an large number of rings behaves like the bulk material.

The limit for the longitudinal velocity approaches almost perfectly the bulk value of 9.35 km/s, which emphasizes the validity of the model used. The value for the transverse sound velocity, on the other hand, is an overestimation of about 20%.

From our calculations we not only obtained frequencies for all modes of the spectrum, but also eigenvectors of the vibrations, i.e., the displacement of all atoms. In Fig. 5 we see the eigenvectors of the four modes around 1.5 THz for  $q=0$ . The Si atoms are depicted by little spheres with glyphs

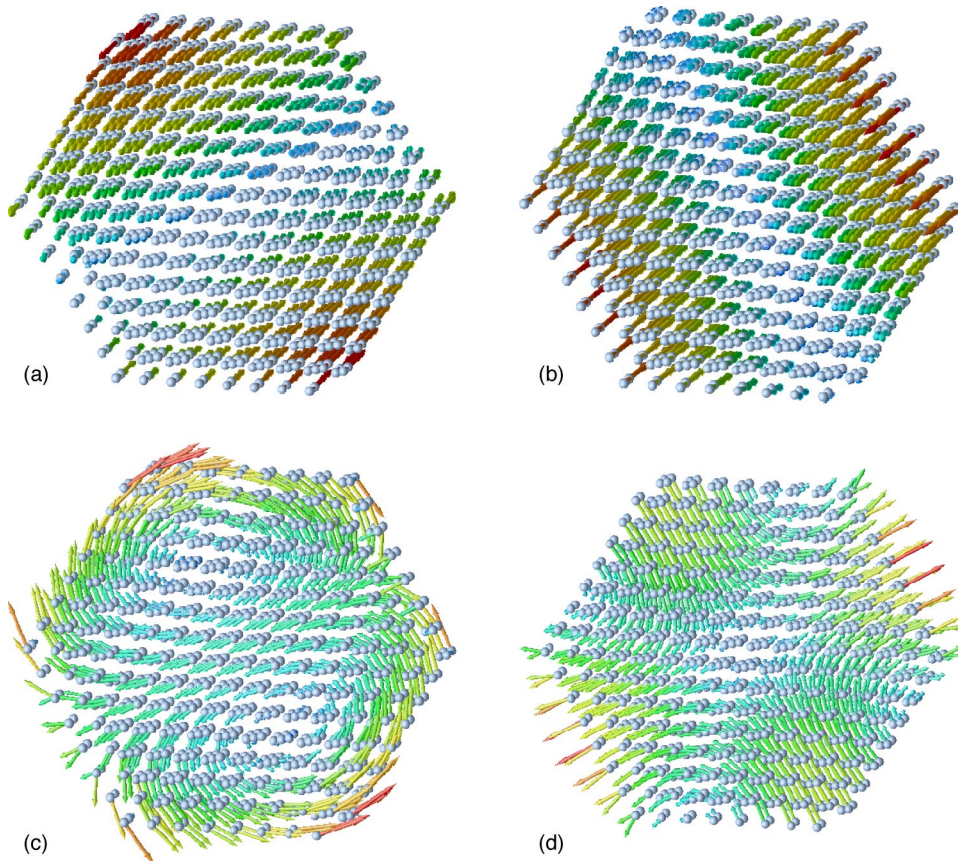


FIG. 5. (Color online) Eigenvectors of the acoustic modes around 1.5 THz for  $q=0$ . The line of sight is slightly off the [111] direction in order to better view the mostly longitudinal modes in (a) and (b).

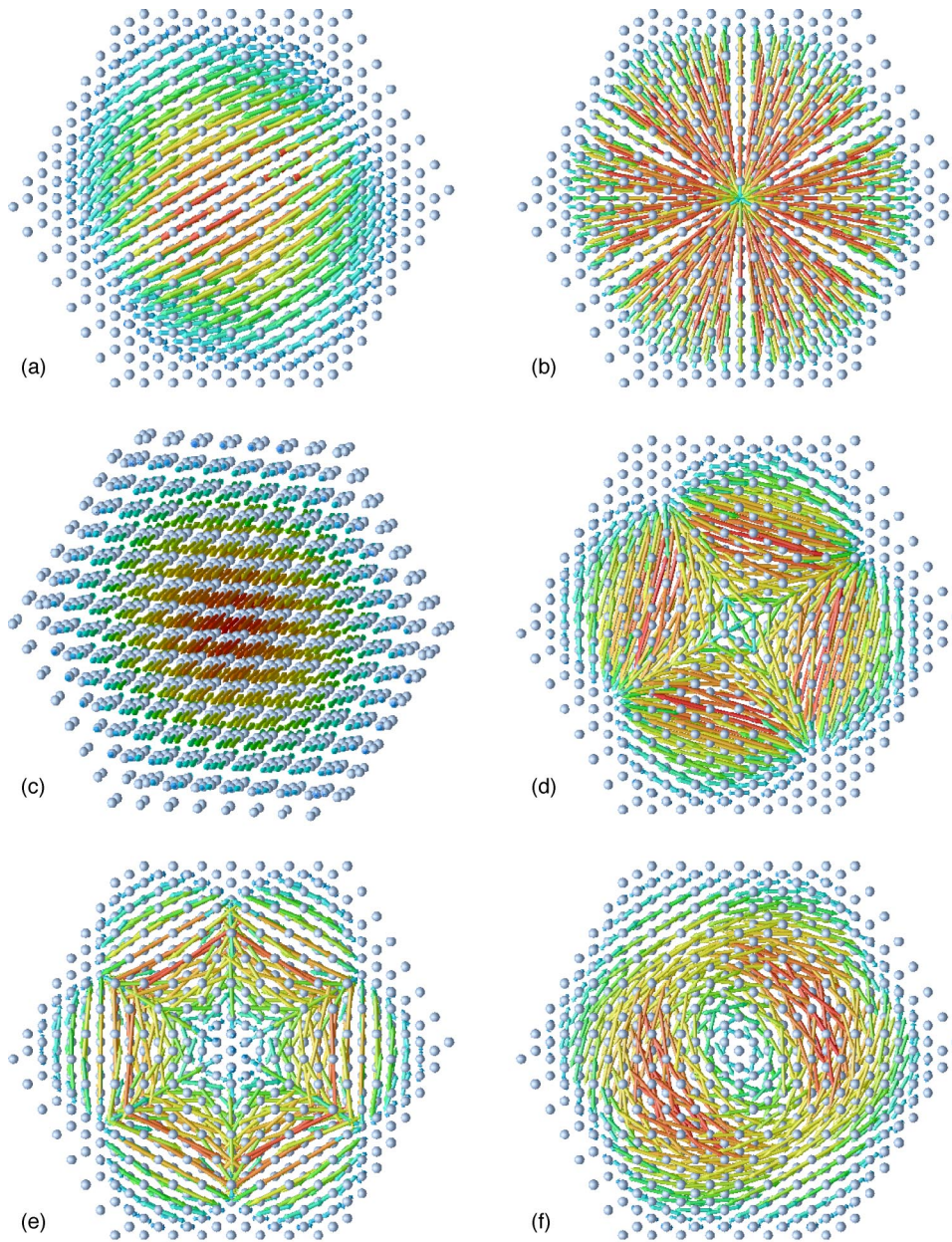


FIG. 6. (Color online) Eigenvectors of some optical phonon modes around 15.3 THz for  $q=0$ . The line of sight parallels the  $[111]$  direction, except in case (c), where it is slightly off the  $[111]$  direction, so that the mostly longitudinal mode is better to see.

indicating their movements according to value and direction. The modes are increasing in frequency from (a) to (d). While the eigenvectors in (a) and (b) are almost exclusively longitudinal, the ones in (c) and (d) are mostly transversal. Eigenvectors for values  $q \neq 0$  look similar to the ones depicted. Note that only modes near the upper and lower frequency boundary of the spectrum are purely optical or purely acoustic. Modes in the region in between are, in general, a superposition of both and the character changes gradually. In Fig. 6 the highest frequency optical phonon modes around 15.3 THz are depicted. For all graphs in this figure the line of sight parallels the  $[111]$  direction, so that the symmetry of the eigenvector becomes more obvious. However, in graph (c) the line of sight is slightly off the  $[111]$  direction in order to better depict the mostly longitudinal solution. It can be seen that, although the opposed symmetry from the wire is sixfold, all kinds of symmetries are present. As for acoustical

phonons, eigenvectors for values  $q \neq 0$  look similar to the ones depicted. All optical modes obey  $\mathbf{Q}=0$  on the surface of the wire, which follows naturally from the solution of Eq. (5), i.e., the dynamical equation<sup>4</sup>. This is also true for modes with  $q \neq 0$ . The result does not depend on the material used and is therefore completely general as long as the diamond structure is utilized. It follows that optical phonon modes in nanowires are subject to clamped boundary conditions. This is different from the boundary conditions found in Fig. 5, where  $\mathbf{Q} \neq 0$  was found on the surface, in accordance to the well-known stress free boundary conditions for acoustical phonons.

## V. CONCLUSIONS

We solve a long standing question concerning the boundary conditions for optical phonons in nanowires by perform-

ing phonon calculations for Si [111] nanowires. Using a spring-and-mass model of the Stillinger and Weber type we solved for the phonon spectrum as well as for the eigenvectors, i.e., the displacement of all atoms, of phonons in free-standing wires of several diameters. The model used is a real crystalline model, whereas previous calculations solved either isotropic models or focused on other systems like embedded wires. Our results for the phonon spectrum and calculated sound velocities emphasize the validity of our approach. The calculated eigenvectors for acoustical phonons are in agreement with the well-known boundary conditions for acoustical modes, i.e., vanishing surface

stress. The eigenvectors for the optical modes reveal that all displacements at the surface of the wire are zero, which means that optical phonons in nanowires are subject to clamped boundary conditions.

#### ACKNOWLEDGMENTS

We would like to acknowledge fruitful discussions with Josh Gladden, Julian D. Maynard, and Peter Eklund. Furthermore, this work was supported by NSF Grant No. DMR-02-05125 and in part by the Materials Simulation Center, a Penn-State MRSEC and MRI facility.

- 
- <sup>1</sup>M. S. Dresselhaus, G. Dresselhaus, and P. C. Eklund, *Science of Fullerenes and Carbon Nanotubes* (Academic Press, New York, 1996).
- <sup>2</sup>M. A. Stroschio and M. Dutta, *Phonons in Nanostructures* (Cambridge University Press, Cambridge, 2001).
- <sup>3</sup>G.D. Mahan, Phys. Rev. B **65**, 235402 (2002).
- <sup>4</sup>B. K. Ridley, *Electrons and Phonons in Semiconductor Multilayers* (Cambridge University Press, Cambridge, 1997).
- <sup>5</sup>C. Trallero-Giner, R. Pérez-Alvarez, and F. Garcia-Moliner, *Long Wave Polar Modes in Semiconductor Heterostructures* (Pergamon, New York, 1998).
- <sup>6</sup>M.A. Stroschio, K.W. Kim, S. Yu, and A. Ballato, J. Appl. Phys. **76**, 4670 (1994).
- <sup>7</sup>B.K. Ridley, Phys. Rev. B **44**, 9002 (1991).
- <sup>8</sup>B.K. Ridley, Phys. Rev. B **47**, 4592 (1993).
- <sup>9</sup>C. Trallero-Giner, F. Garcia-Moliner, V.R. Velasco, and M. Cardona, Phys. Rev. B **45**, 11 944 (1992).
- <sup>10</sup>M. Babiker, J. Phys. C **19**, 683 (1986).
- <sup>11</sup>A. E. H. Love, *A Treatise on the Mathematical Theory of Elasticity* (Dover, New York, 1944).
- <sup>12</sup>P. M. Morse and H. Feshbach, *Methods of Theoretical Physics* (McGraw-Hill, New York, 1953).
- <sup>13</sup>L. D. Landau and E. M. Lifshitz, *Theory of Elasticity* (Addison-Wesley, Reading, MA, 1959).
- <sup>14</sup>G.D. Mahan, R. Gupta, Q.H. Xiong, C.K. Adu, and P.C. Eklund, Phys. Rev. B **68**, 073402 (2003).
- <sup>15</sup>P.N. Keating, Phys. Rev. **145**, 637 (1966).
- <sup>16</sup>F.H. Stillinger and T.A. Weber, Phys. Rev. B **31**, 5262 (1985).
- <sup>17</sup>*Numerical Data and Functional Relationships in Science and Technology*, edited by O. Madelung, M. Schulz, and H. Weiss, Landolt-Börnstein, New Series, Group III, Vol. 17 (Springer, New York, 1983).
- <sup>18</sup>N. W. Ashcroft and N. D. Mermin, *Solid State Physics* (Harcourt College, New York, 1976).